

Synthesis and catalytic evaluation of magnetically recyclable CaO/CoFe₂O₄ nanoparticles for biodiesel production via ethylic transesterification

Diogo Gontijo Borges^{1*}, Audrey Moores² and José Mansur Assaf¹

¹Laboratory of Catalysis, Department of Chemical Engineering, São Carlos Federal University, C. Postal 676, CEP: 13565-905, São Carlos-SP, Brazil.

²Center for Green Chemistry and Catalysis, Department of Chemistry, McGill University, H3A-0B8, Montreal-QC, Canada.

Corresponding Author: Diogo Gontijo Borges

ABSTRACT: CaO/CoFe₂O₄ nanoparticles were easily synthesized by calcination at 650°C for 1h of Ca(NO₃)₂·4H₂O impregnated CoFe₂O₄ nanoparticles. The resulting systems were studied as catalysts for the transesterification reaction of esters with ethanol under mild reaction conditions (70°C, ethanol/ester molar ratio = 6/1 and 4 wt.% of catalyst, at 30, 60, 120, 180 and 240 min). For this reaction, methyl acetate and soybean oil were tested as substrates, and the effect of reaction time and ester/ethanol ratio on performance was studied. The materials were characterized by XRD, SQUID, N₂ physisorption, TEM equipped with energy-dispersive X-ray spectroscopy (EDX), XRF, and CO₂-TPD. Optimized catalyst and reaction conditions afforded in 4 h 68% conversion for methyl acetate and 29% for soybean. The proposed catalysts were magnetically separated and reused for the same reaction in up to 6 cycles. Ca²⁺ was shown to leach, but did not afford any homogeneous catalytic activity. As such, the CaO/CoFe₂O₄ catalysts showed promise for replacing alkaline homogeneous catalysts for biodiesel production.

KEYWORDS: Biodiesel, Transesterification reaction, Calcium oxide, Cobalt ferrite, Heterogeneous base catalyst.

Date of Submission: 16-01-2019

Date of acceptance: 28-01-2019

1. INTRODUCTION

The search for renewable energy sources has attracted global interest and in recent years, there has been increasing research into replacing fossil fuels. Fossil fuels generate pollutants and are linked to global warming, climate change and even to the increasing frequency of the appearance of some serious diseases. The looming challenges of substitution and the environmental implications of the use of fossil fuels have been extensively discussed in the literature (Aransiola *et al.*, 2014). Biodiesel is important option for conventional fuels abatement. It is primarily produced via transesterification reactions, also known as alcoholysis of vegetable and/or animal fats, or by esterification of free fatty acids by use of an acid, basic or enzymatic catalyst (Mardhiah *et al.*, 2017). Biodiesel is compatible with current diesel-cycle engine technology, making it as an alternative technique able to immediately attended to all existing fleets already powered by petroleum diesel. Biodiesel also provides a number of environmental advantages compared to petroleum-based diesel such as low carbon monoxide and particulate matter emissions during combustion, no sulfur compound emissions into the atmosphere, better fuel properties, such as cetane number and lower emissions of the main greenhouse gases because the carbon dioxide produced in the combustion is almost totally consumed during cultivation of the oilseeds (Mardhiah *et al.*, 2017; Goet *et al.*, 2016; Cordeiro *et al.*, 2011).

Both homogeneous and heterogeneous catalysts have been developed for these technologies, relying on either strong base or strong acid catalysis (Hasan and Rahman, 2017). Conventionally homogeneous catalysts are used but suffer from several disadvantages in the process, including the generation of wastewater produced during the cleaning of the product and the difficulty in operating a continuous process (Tang *et al.*, 2013). Many heterogeneous catalysts, such as alkali metal hydroxides and oxides, have shown significant levels of conversion in such reactions. Among these basic heterogeneous catalysts, calcium oxide (CaO) stands out for its low cost, simple preparation and high activity under mild reaction conditions (Nair *et al.*, 2012). However, some research showed that CaO featured low stability in the reaction system (Gryglewicz, 1999). Researchers found that the CaO dissolved readily in alcoholic solution and was difficult to separate and recover from the reaction mixture (Kouzu *et al.*, 2009). To circumvent these problems, CaO supported on different arrays were investigated in order to increase the stability, allowing catalyst reuse (Shi *et al.*, 2017; Bet-Moushoulet *et al.*, 2016; Castro *et al.*, 2014).

Important research efforts have been focused on the development of magnetic nanoparticles in catalysis, as they offer a unique avenue for easy separation technologies (Rossi *et al.*, 2014; Polshettiware *et al.*, 2011; Lu, Salabas, Chem, 2007). In this scheme, strategies include the grafting of homogeneous catalysts at the surface of the magnetic nanoparticles, the deposition of catalytic materials on its surface, or the direct use of the magnetic nanosized materials as catalysts (Hudson *et al.*, 2014). In all cases, magnetic nanoparticles combine the high surface-over-volume ratio, allowing a high density of catalytic sites, which the magnetic properties making them tractable using an external magnet (Huixia *et al.*, 2014), thereby facilitating removal of the catalyst from the reaction system and eliminating filtration step. In this context, ferrite nanoparticles (MFe₂O₄) are appealing materials combining magnetic properties, easy synthesis, versatile crystalline form groups: cubic or spinel and hexagonal ferrites or hexaferrites (Arana *et al.*, 2013; Mozaffari *et al.*, 2014), and the ability to modulate properties by careful choice of complementary metal M. Among these nanoparticles, the cobalt ferrite (CoFe₂O₄), which has a cubic spinel structure, is emphasized due to its high coercivity, moderate saturation magnetization, high stability and elevated mechanical strength (Huixia *et al.*, 2014), becoming a promising material in the development of magnetic catalysts.

In this paper, we present the simple synthesis of novel magnetic nanoparticles active for the ester transesterification. We deposited onto cobalt ferrite nanoparticles, used here as magnetic cores, calcium oxide as a heterogeneous alkaline transesterification catalysts. The catalysts were evaluated for the transesterification reaction of either methyl acetate or soybean oil with ethanol.

2. EXPERIMENTAL

2.1. Catalysts preparation

The cobalt ferrite nanoparticles was synthesized according to the methodology described by Borges (2015). 4 mmol of Fe(NO₃)₃·9H₂O, 2 mmol of Co(NO₃)₂·6H₂O and 9 mmol of citric acid were dissolved in 50 mL of distilled water. The solution was heated at 90°C in a silicone bath under continuous stirring till removal of water excess, forming a high viscosity precursor citrate. The temperature was increased to 300°C for the citric acid decomposition, causing the expansion of the precursor due to the entrapment of the carbon monoxide, carbon dioxide and water vapor gases, resulting in a semi-carbonised, black and brittle foam, called "puff".

The material obtained above was used as solid support for calcium oxide addition by the wet impregnation method. Ca(NO₃)₂·4H₂O was dissolved in 20 mL of ethanol and then cobalt ferrite added. The suspension was stirred at 80°C until complete solvent evaporation. Catalysts were prepared with different loadings of CaO: 10, 20, 30, 40 and 50 wt.% (wt. of Ca²⁺ cobalt ferrite support). Subsequently, calcination at 650°C/1h was performed on the recovered powders and were named CoFe₂O₄ and X-CaO/CoFe₂O₄, in which "X" is the calcium loading in wt.%.

2.2. Characterization

2.2.1. X-ray diffraction (XRD)

The catalysts were characterized by X-ray diffraction at room temperature in a Rigaku Multiflex equipment using Cu-K α radiation ($\lambda = 1.5406 \text{ \AA}$) with a scan range 2θ angles from 3 to 80° 0.02° step and goniometer rate of 2°·min⁻¹. The obtained data were compared with JCPDS files database.

2.2.2. Transmission electron microscopy (TEM) and Energy Dispersive X-ray Spectroscopy (EDX)

The oxide morphologies and elemental chemical analysis were studied by transmission electron microscopy (TEM) equipped with Energy Dispersive X-ray Spectroscopy (EDX). The images were obtained in a FEI Tecnai G20F20 electron microscope.

2.2.3. Nitrogen adsorption/desorption analysis

Nitrogen physisorption at 77 K was used for surface area determination on a NOVA-1200 Quantachrome equipment by using the Brunauer–Emmett–Teller (BET) method.

2.2.4. X-ray fluorescence spectrometer (XRF)

The Ca concentrations supported on CoFe₂O₄ were determined by X-ray fluorescence spectrometry (XRF) on a Shimadzu EDX-720, RayNy.

2.2.5. Temperature programmed desorption technique (CO₂-TPD)

The catalyst basicity was evaluated by the temperature programmed desorption technique (CO₂-TPD). The samples (100 mg) were heated at a rate of 20°C min⁻¹ until the calcination temperature of 650°C for 1h under a helium atmosphere flow of 50 mL·min⁻¹ to remove the adsorbed impure species. CO₂ adsorption was then performed at 100°C for 5 minutes using a CO₂ flow of 50 mL·min⁻¹. This was followed by helium purge to remove physically adsorbed CO₂. The CO₂ desorption amount was then measured by a TCD detector by heating

the samples at a rate of 50°C min⁻¹ under helium atmosphere (flow of 30 mL.min⁻¹) until 1000 °C.

2.2.6. Magnetic measurements

The magnetic measurements of the catalysts were performed in a Superconducting quantum interference device (SQUID). The magnetometry measurements were carried out using a Quantum Design MPMS XL magnetic property measurement system. Each powder sample was loaded in a gelatin capsule, which was sealed with a thin strip of Kapton tape. The capsule was inserted in a clear plastic straw fixed to the MPMS sample rod. Centering of the samples was done under zero field. For both zero-field-cooled (ZFC) and field-cooled (FC; applied field was 10 mT) measurements, the samples were first cooled to -254°C before allowed to warm up to 127°C under 10 mT while magnetization was measured. ZFC measurement precedes FC. Finally, magnetic hysteresis loops were measured at temperatures of 27 and -254°C, with applied field up to 7 T or the minimum needed for saturation.

2.2.7. Atomic Absorption Spectroscopy

The determination of possible calcium leaching from the catalysts was carried out by chemical analysis of the reaction solution. For this purpose, the supernatant solution was collected after reaction and the catalyst was removed by filtration using syringe filters (0.45 µm pore size). Thus, the volatiles were evaporated and re-suspended with 1% (v/v) HNO₃ solution for chemical analysis of residual calcium. The calcium content in the solution was analyzed by atomic absorption spectroscopy (Varian Spectr AA).

2.2.8. Temperature-programmed Desorption of CO₂ (CO₂-TPD)

The catalysts basicity was evaluated by the Temperature-programmed CO₂ desorption technique (CO₂-TPD). First, 100 mg of sample was subjected to a pretreatment using a heating rate of 20°C min⁻¹ until 650°C for 1 hour under a helium atmosphere with a flow of 50 mL min⁻¹ to remove adsorbed impurities. The sample was cooled to 100°C and CO₂ adsorption performed for 1 hour using a CO₂ flow rate of 50 mL min⁻¹. Subsequently, the system was purge with He for 1 hour to remove the adsorbed CO₂. The sample was cooled to 50°C and the CO₂ desorption was then performed under He flow at 30 mL.min⁻¹, by heating samples at a rate of 50°C min⁻¹ up to 1000°C. The desorbed CO₂ was detected using a thermal conductivity detector (TCD). The results were obtained by integration and the areas under the CO₂-TPD curves using Gaussian functions.

2.3. Catalysts evaluation

Experiments were carried out in 2 mL micro-reactors as described by Martins (2007). Methyl acetate was chosen as a simple model reagent for screening the active catalysts for transesterification. A solution containing a 6/1 ethanol/methyl acetate (molar ratio) was placed in contact with 4% of catalyst (wt. catalyst/wt. of the reaction mixture) at 70°C controlled by immersion of the reactor in hot water in a reaction time of 30, 60, 120, 180 and 240 min. In the end of the run, the reactions were stopped by immersing the reactor in an ice bath. The catalyst was separated and the supernatant recovered for product analysis by GC (GC Varian Star Model 3400) equipped with a FID detector and an RTx[®]-1 capillary column.

Upon completion of the transesterification using model molecules, a catalytic test was performed using soybean oil (Molar mass = 874.8 g/mol) and ethanol. The reaction was carried under the same test conditions on model molecules while maintaining the 4% (w/w) ratio of the catalyst and varying the ethanol/soybean oil ratio 6/1, 12/1 and 24/1. The conversion was analyzed at four different reaction times: 4; 8; 12 and 24 h. After each reaction time, an aliquot was withdrawn from the reactor and decanting was conducted. Three phases were obtained: a solid containing the catalyst, a heavy liquid phase mainly comprised of glycerine and ethanol and a light liquid phase consisting of esters and ethanol. The solid phase was removed and the other two phases formed were washed with warm water. An aliquot of the light/organic liquid phase was analyzed by GC, in order to determine the content of esters produced and separated at this stage of interest. The standard used to determine the ester content was the European standard - EN 14103. This is the Standard: Fatty Acid Methyl Esters (FAME) - Determination of ester and linolenic acid methyl ester contents.

2.4. Stability evaluation

The catalyst stability investigation was carried out using different methods. Primarily, the catalyst stability was investigated using the methodology proposed by Sheldon *et al.* (1998) and Braga *et al.* (2011), which consists of removing the catalyst from the reaction system after 1 h of reaction and subsequently monitoring the composition of the remaining solution under same reaction conditions without the catalyst, for 3 hours.

The catalyst recyclability was also tested. The experiments were performed in 2 mL micro reactors under the same conditions described for the catalytic tests. After 2 h of reaction, the catalyst was separated magnetically using neodymium magnet from reaction solution. Knowing that the CaO is carbonated and easily

hydrated in contact with atmospheric CO₂ and H₂O, the recovered catalysts were not dried and kept in contact with a minimum quantity of reactants and products, before a new reaction mixture was added for carrying out an additional cycle.

3. RESULTS AND DISCUSSION

3.1. Support and catalysts characterization

CoFe₂O₄ and CaO/CoFe₂O₄ nanoparticles were characterized by X-ray diffraction (XRD, Figure 1-a). The diffraction peaks of the CoFe₂O₄ (JCPDS 077-0426) with cubic structure were observed in all samples. CaO/CoFe₂O₄ samples featured diffraction peaks characteristic of CaO, of raising intensity as the CaO/CoFe₂O₄ ratio increased. The 10-CaO/CoFe₂O₄ sample presented characteristic features of CoFe₂O₄, with the CaO formed suggesting that this sample has a small crystallite size (Figure 1-a). In the 20-CaO/CoFe₂O₄ sample, the intensity of the peaks related to CaO can be observed, consequently the peaks increase intensity are easily observed in the 30-CaO/CoFe₂O₄, 40-CaO/CoFe₂O₄ and 50-CaO/CoFe₂O₄ samples (Figure 1-a).

Due to the fast CaO hydration and carbonation in atmospheric air, diffraction peaks characteristic of Ca(OH)₂ (JCPDS 72-0156) and CaCO₃ (JCPDS 85-1108) were detected. Similar patterns were seen in the diffractogram obtained from commercial CaO (Figure 1-b).

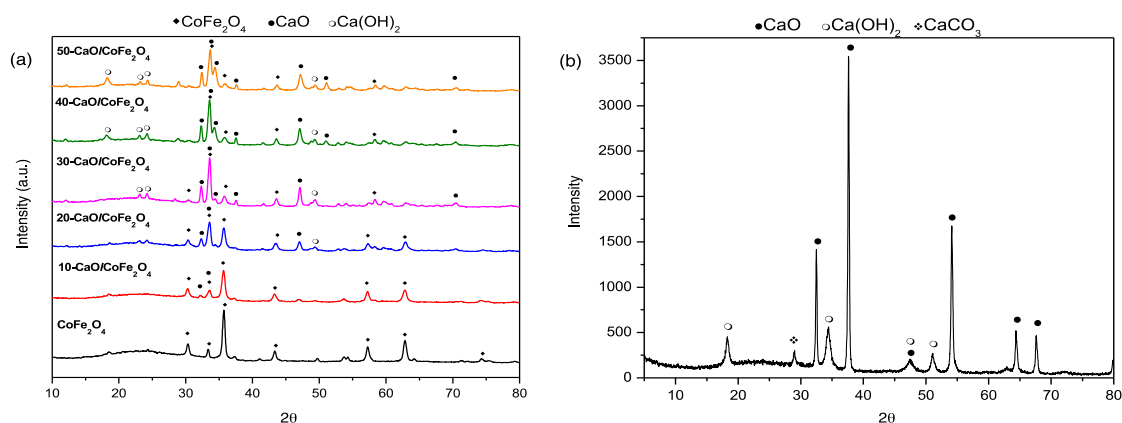


Figure 1. X-ray diffractogram for CoFe₂O₄ and X-CaO/CoFe₂O₄ (a) and commercial CaO (b).

The morphology of the nanocatalysts was studied by transmission electron microscopy (TEM). CoFe₂O₄ nanoparticles appear as faceted nanoparticles of diameter ranging from 20 to 60 nm (Figure 2-a). Sample 10-CaO/CoFe₂O₄ and 20-CaO/CoFe₂O₄ (Figures 2-b) looked very similar to the sample without CaO, in terms of both size and morphology. Figures 2-d and 2-e show the micrographs of the catalysts, 30-CaO/CoFe₂O₄ and 50-CaO/CoFe₂O₄, respectively. With increased CaO content, the observed nanoparticles increased in size drastically, suggesting that CaO covered the surface of the ferrite nanoparticle and possibly merged several CoFe₂O₄ nanoparticles together. The chemical analysis of the sample surfaces was made by EDX (Figure 2 f-j). Ca-characteristic peaks were seen for all CaO-impregnated samples. Their intensity increased as a function of CaO content.

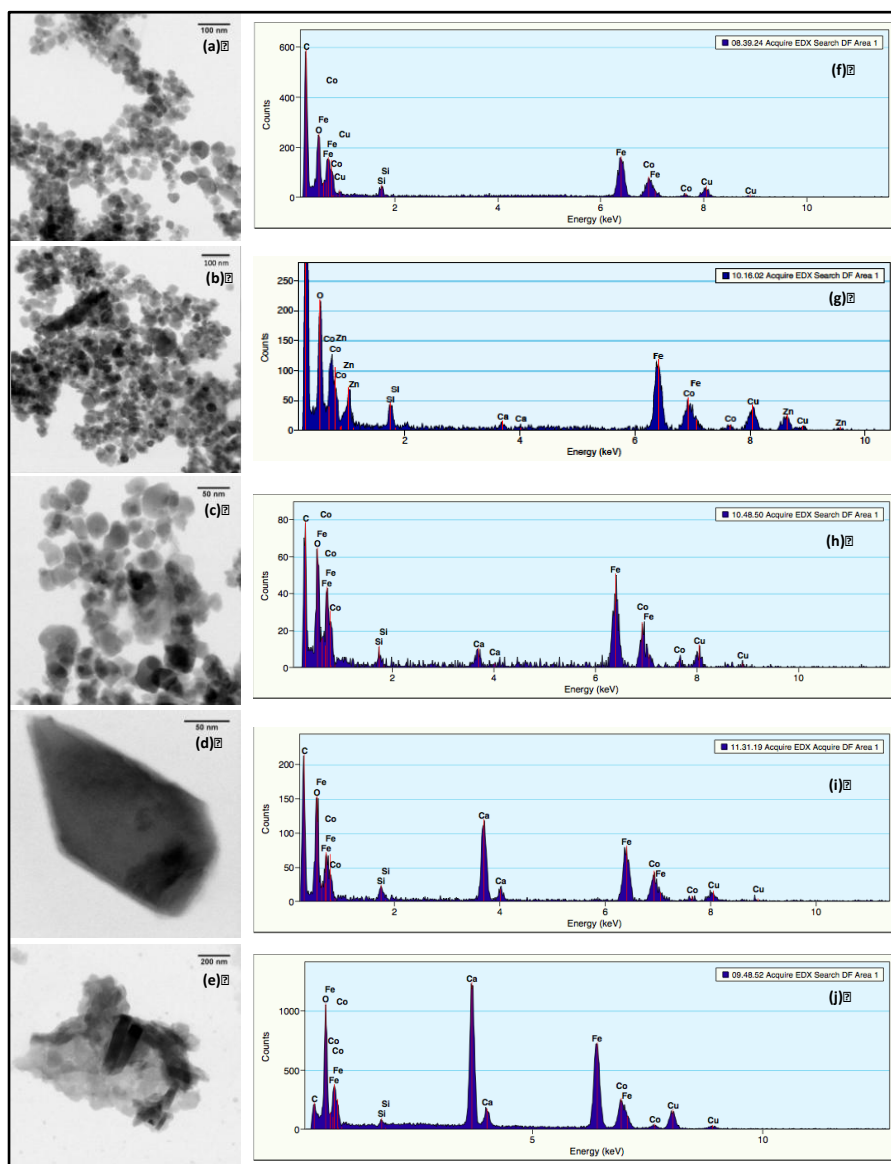


Figure 2. TEM of CoFe₂O₄ (a); 10-CaO/ CoFe₂O₄ (b), 20 CaO/ CoFe₂O₄ (c), 30-CaO/ CoFe₂O₄ (d) and 50-CaO/ CoFe₂O₄ (e) Spectra and energy dispersive X-ray (EDX) of the micrographs shown left (f-j).

Table 1 presents the specific area values of all synthesized catalysts, determined by BET method. CoFe₂O₄ featured a specific surface area value of 34 m².g⁻¹. This BET value is consistent with the specific surface of nanoparticles of the size range observed by TEM. 10-CaO/CoFe₂O₄ featured a very similar specific area, which is consistent with the deposition of small CaO nanoparticles. With increasing CaO content, a significant decrease in the area values occurred. It dropped by 3.6 times for 20-CaO/CoFe₂O₄ and then dropped below 1 m².g⁻¹ for samples X-CaO/CoFe₂O₄ (X=30, 40 and 50).

Table 1- Specific area for the catalysts determined by BET.

Catalysts	BET area (m ² .g ⁻¹)
CoFe ₂ O ₄	34
10- CaO/CoFe ₂ O ₄	35
20- CaO/CoFe ₂ O ₄	9.4
30- CaO/CoFe ₂ O ₄	<1
40- CaO/CoFe ₂ O ₄	<1
50- CaO/CoFe ₂ O ₄	<1
CaO	3

Table 2 displays the chemical analysis determined by X-ray fluorescence (XRF) for CaO/CoFe₂O₄. These results showed that the levels determined experimentally were close to nominal levels. The differences observed are possibly due to the intrinsic error in hydrate content in starting materials and losses during the impregnation and subsequent drying stages.

Table 2 - Ca content determined by X-ray Fluorescence catalysts CaO / CoFe₂O₄.

Catalysts	Nominal content (% wt/wt)	Experimental content (% wt/wt)
10- CaO/CoFe ₂ O ₄	10	11.5
20- CaO/CoFe ₂ O ₄	20	21.4
30- CaO/CoFe ₂ O ₄	30	33.8
40- CaO/CoFe ₂ O ₄	40	40.6
50- CaO/CoFe ₂ O ₄	50	45.0

Figure 3 and Table 3 show the CO₂-TPD patterns obtained from catalysts investigated in this paper. It can be observed that CoFe₂O₄ and 10-CaO/CoFe₂O₄ samples showed the same characteristic for both materials, which can be attributed to the interaction of CO₂ with medium-strength basic sites (Braga *et al.*, 2011).

Table 3-Density of basic sites for catalysts X-CaO/CoFe₂O₄.

Catalysts	Density of basic sites- db (μmol/m ²)		
	Weak db	Strong db	Total db
CoFe ₂ O ₄	1.9	-	1.9
10-CaO/CoFe ₂ O ₄	-	-	0
20-CaO/CoFe ₂ O ₄	0.6	-	0.6
30-CaO/CoFe ₂ O ₄	-	2.3	2.3
50-CaO/CoFe ₂ O ₄	-	9.5	9.5

Increasing of the calcium content on the samples leads to the disappearance of this band, suggesting that CaO particles are covering the CoFe₂O₄ surface, as shown in Figure 2. The appearance of CO₂ desorption bands at higher temperatures indicates that increasing the calcium amount incorporated into the catalysts generated stronger basic sites. Taufiq-Yap *et al.* (2011) reported that the intense band between 400-650°C is related to Ca²⁺O²⁻ pairs that have high basic strength. The results show that the addition of calcium contributed to the development of strong basic sites which were quantified by density analysis of basic sites in proportion to the amount of CO₂ desorbed from the catalyst.

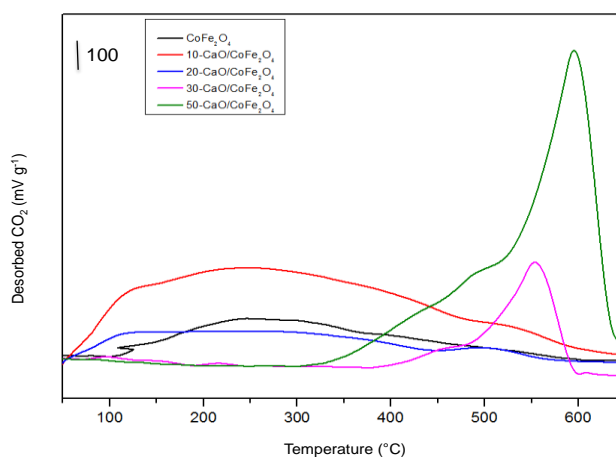


Figure 3. TDP-CO₂ patterns of CoFe₂O₄, 10-CaO/CoFe₂O₄, 20-CaO/CoFe₂O₄, 30-CaO/CoFe₂O₄ and 50-CaO/CoFe₂O₄.

The magnetization curves, as shown in Figure 4, were obtained for samples CoFe₂O₄ and 50-CaO/CoFe₂O₄. The measurements were performed at 27 and -254°C. The magnetization curves at 27°C, show that both samples present excellent magnetic properties, reaching saturation magnetization values of about 30

emu/g and superparamagnetic material properties (remanent magnetization and coercivity are zero).

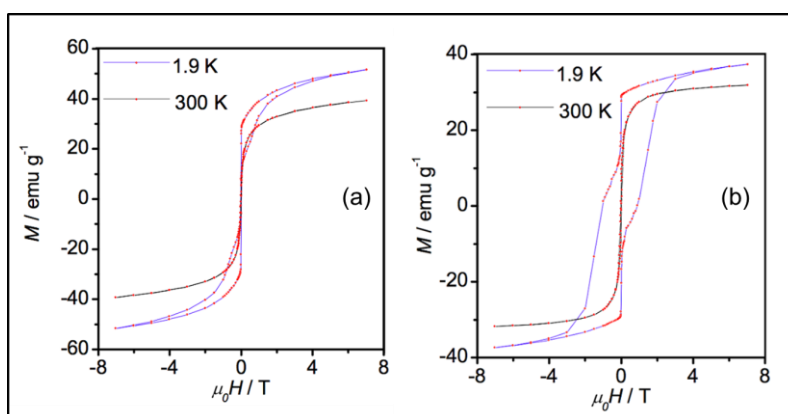


Figure 4. Magnetization curve for samples CoFe₂O₄ (a) and 50-CaO / CoFe₂O₄ (b).

As expected, hysteresis curves determined at -254°C are distinctly different from measurements performed at 27°C. At -254°C, both materials exhibit coercivities and remanent magnetization, being directly related to the magnetic anisotropy of the material. This is because at low temperatures the magnetic anisotropy increases. Therefore, the lower the temperature, the higher the magnetocrystalline anisotropy constant of the material (Grigorova, 1998).

Importantly, all the materials used in this paper presented superparamagnetic behavior, meaning they were strongly attracted to a magnetic field, but also no residual magnetization, meaning that their magnetization dropped to zero, as soon as field vanished. Both features are important for efficient magnetically recoverable catalysts (Chien, 1991).

3.2. Catalytic evaluation

The catalytic activity of the designed materials was evaluated for the model transesterification reaction between methyl acetate and ethanol at 70°C with ethanol/ester molar ratio of 6/1 and 4 wt.% of catalyst with reaction times varying from 30 min to 4 hours (Figure 5).

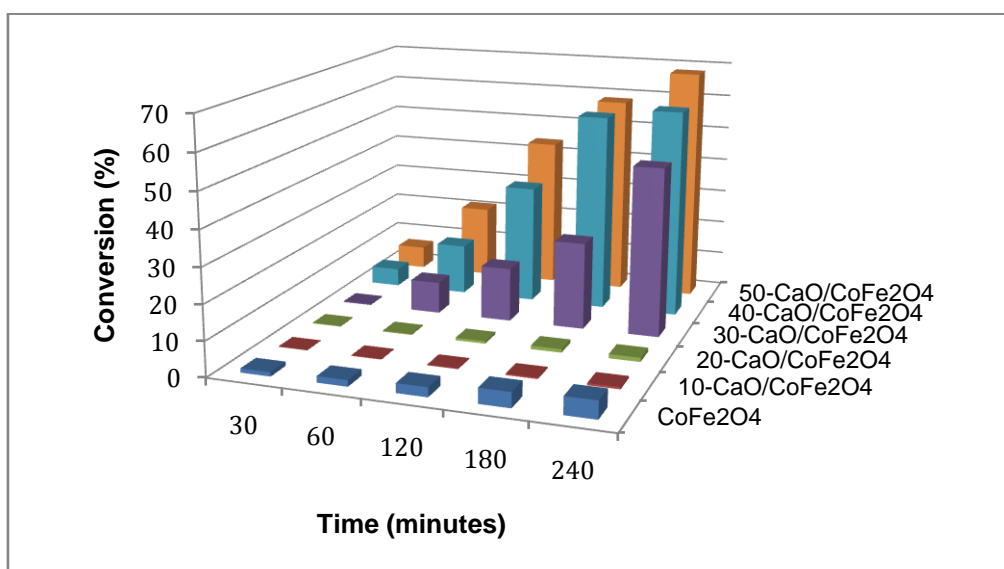


Figure 5. Catalytic test for transesterification reaction between model molecules in the time between methyl acetate and ethanol.

CoFe₂O₄ nanoparticles showed marginal yield rates of 5% at 4 hours of reaction. This residual activity was possibly linked to the synthetic method, where alkaline solution (NaOH) were used during the precipitation step. 10-CaO/CoFe₂O₄ and 20-CaO/CoFe₂O₄ showed no conversion, even after 4 h of reaction. Significant activity boost was observed when CaO content was increased. For instance, 30-CaO/CoFe₂O₄ afforded 49% conversion, 40-CaO/CoFe₂O₄ 61%, and 50-CaO/CoFe₂O₄ 68%, respectively, after 4 hours. Based on this, we can infer that the increased concentration of CaO supported on CoFe₂O₄ is essential for the creation of active

sites for the reaction, and the ferrite plays an auxiliary role in the dispersion and stabilization of the active phase (CaO).

The catalysts performance may be explained by considering the textural properties of the catalysts as well as the basicity. The catalytic activity depends on the Ca²⁺ content, which affects the amount and strength of basic sites, plus the physical properties of the catalysts, mainly specific area and crystallite size of the active phase of CaO (Demirbas, 2008).

Because of its excellent catalytic performance, catalyst 50-CaO/CoFe₂O₄ was tested in the transesterification reaction of soybean oil with ethanol. Conversion to the corresponding methyl-ester is presented Figure 6, as a function of reaction time and soybean/ethanol oil ratio. The reaction progressed quasi linearly as a function of time reaching 13% after 24 hours with the ethanol/soybean ratio of 6/1. Raising this ratio to 24/1, the conversion improved to 29% after 24 hours. This trend can be explained by the fact that the transesterification of vegetable oils is kinetically favored when an excess of alcohol is used relative to the triglyceride. We did not explore ethanol:soybean oil ratios above 24/1, as large excess of ethanol interferes with glycerol separation due to the increase in its solubility of glycerol in ethanol. Furthermore, the presence of glycerol in the reaction system favors the formation of triglycerides (Demirbas, 2008).

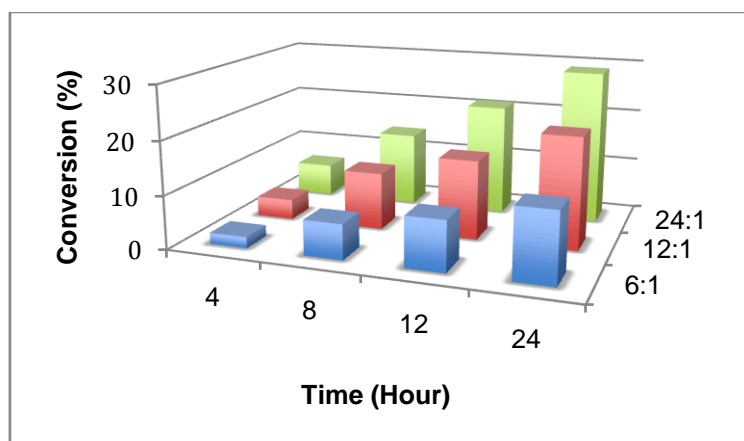


Figure 6. Catalytic evaluation of 50-CaO/CoFe₂O₄ catalyst for the transesterification between soybean oil and ethanol.

The obtained maximum conversion was 29%. It is relatively low when compared to the 68% conversion in the reaction performed using model molecules. This result may be attributed to the greater complexity of the triglycerides present in soybean oil when compared with methyl acetate used in the model reaction. This influences the complexity of molecule connections between the triglycerides and the active sites of the catalyst, resulting in a lower reaction rate, since less triglyceride molecules can bind to sites (Castro *et al.*, 2014).

3.3. Catalyst stability

Considering that the present study aims at the production of heterogeneous catalysts for use in liquid-phase reactions, the stability study becomes necessary. The loss of the active phase for the reaction system by leaching is a major obstacle in the production of heterogeneous catalysts, since these leached species can be solubilized in the liquid system, homogeneously catalyzing the reaction and contaminating of the final product, while revealing a degradation of the catalysts.

The reuse of the 50-CaO/CoFe₂O₄ catalyst was investigated in six consecutive runs at 70°C, ethanol/ester molar ratio=6/1 and 4 wt.% of catalyst for 2h (Figure 7). After the reaction, the catalyst was magnetically sequestered and the supernatant was removed. A new reaction mixture was placed in contact with the catalyst used. The yield is showing how relative conversion, being offered for the first cycle 100% yield and losing a yield on reuse. Over the 6 cycles, the relative conversion dropped 41%.

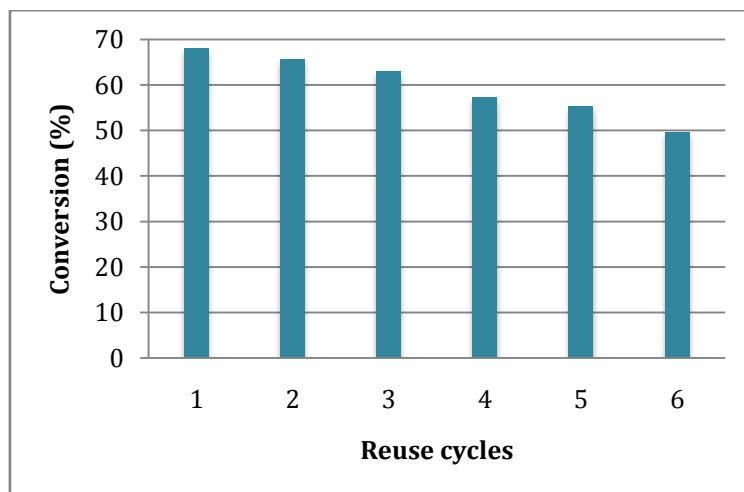


Figure 7. Reuse cycles for catalyst 50-CaO/ CoFe₂O₄

Based on this activity loss, we evaluated after each use cycle soluble Ca²⁺ content into the reaction mixture, using Atomic Absorption Spectrometry to determine the (Table 4).

Table 4- Determination of Ca²⁺ leached into the reaction medium by Atomic Absorption Spectrometry.

Reuse cycles	Ca ²⁺ concentration (mg mL ⁻¹)
1	0.10
2	0.08
3	0.09
4	0.09
5	0.11
6	0.10

Ca²⁺ concentrations ranging from 0.08 to 0.11 mg.mL⁻¹ were measured after each cycles. This value remains fairly stable over the different cycles, and this leaching did not impact catalytic activity. Since leached Ca²⁺ was detected in the reaction, it was important to investigate whether these cations in solution form active species capable of catalyzing the reaction in homogeneous phase. To test this hypothesis, a methodology proposed by Sheldon *et al.* (1998) was performed. After 1 hour of reaction, magnetic removal of CaO/CoFe₂O₄ completely stopped activity, because the production concentration remained constant, keeping the conversion unchanged. Thus confirming a purely heterogeneous mechanism (Figure 8).

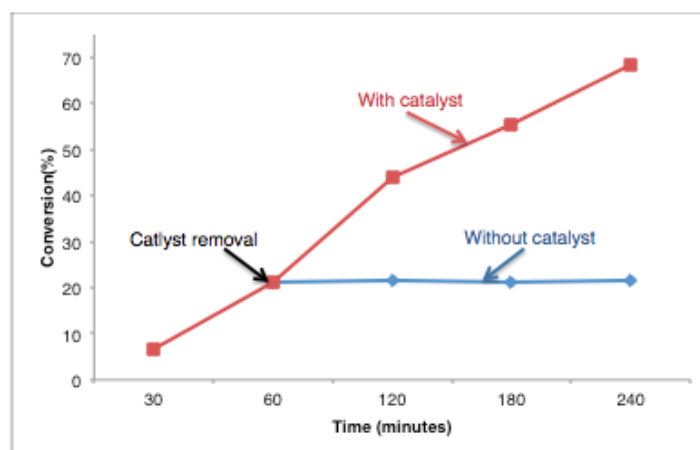


Figure 8. Transesterification reaction in the presence of 50-CaO/ CoFe₂O₄ as a function of the time and after catalyst separation from the reaction system.

4. CONCLUSIONS

It was shown that CoFe₂O₄ nanoparticles used as support facilitates the separation and dispersion of CaO as the catalytically active phase in ester transesterification. Their excellent magnetic properties allowed its easy

separation from the reaction medium by the application of an external magnetic field. The content increase of CaO dispersed on the support was proved fundamental for catalytic activity. The more abundant the CaO, the higher the activity. The 50-CaO/CoFe₂O₄ catalyst showed high conversion (68%) with model molecules and was subsequently applied in the reaction between ethanol and soybean oil showing conversion was 29%. The CaO/CoFe₂O₄ catalyst reuse tests showed that it is feasible to reuse up to 6 times. The CaO/CoFe₂O₄ catalyst can be considered a promising heterogeneous catalyst that may replace homogeneous catalysts for biodiesel production via ethylic transesterification.

5. REFERENCES

Arana, M.; Galván, V.; Jacobo, S. E.; Bercoff, P. G. Cation distribution and magnetic properties of LiMnZn ferrites. *Journal of Alloys and Compounds*, 568, 5–10 (2013).

Aransiola, E. F.; Ojumu, T. V.; Oyekola, O. O.; Madzimbamuto, T. F.; Ikhu-Omoregbe, D. I. O. A review of current technology for biodiesel production: State of the art. *Biomass and Bioenergy*, 61, 276-297 (2014).

Bet-Moushoul, E.; Farhadi, K.; Mansourpanah, Y.; Nikbakht, A. M.; Molaei, R.; Forough, M. Application of CaO-based/Aunanoparticles as heterogeneousnanocatalysts in biodiesel production. *Fuel*, 164, 119-127, (2016).

Borges, D.G. Síntese e caracterização de catalisadores de óxido de cálcio suportado em ferritas magnéticas avaliados na reação de transesterificação etílica. Ph.D. Thesis, Federal University of São Carlos (2015).

Braga, T.P.; Sales, B. M. C.; Pinheiro, A. N.; Herrera, W.T.; Baggio-Saitovitch, E.; Valentini, A. Catalytic properties of cobalt and nickel ferrites dispersed in mesoporous silicon oxide for ethylbenzene dehydrogenation with CO₂. *Catalysis Science and Technology*, 1, 1383–1392 (2011).

Castro, C. S.; Júnior, L. C. F. G.; Assaf, J. M. The enhanced activity of Ca/MgAl mixed oxide for transesterification. *Fuel Processing Technology*, 125, 73–78 (2014).

Chien, C. L. *Science and Technology of Nanostructured Magnetic Materials*. edited Hadjipanayis, G. C.; Prinz, G. A. NATO Advanced Study Institute, Series B: Physics, 259, 477 (1991).

Cordeiro, C. S.; da Silva, F.R.; Wypych, F.; Ramos, L.P. Catalisadores Heterogêneos Para A Produção De Monoésteres Graxos (Biodiesel). *Química Nova*, 34, 477-486 (2011).

Demirbas A. Comparison of transesterification methods for production of biodiesel from vegetable oils and fats. *Energy Conversion and Management*, 49, 125-130 (2008).

Go, A. W.; Sutanto, S. S.; Ong, L. K.; Tran-Nguyen, P.; Ismadji, S.; Ju, Y. Developments in *in-situ* (trans) esterification for biodiesel production: A critical review. *Renewable and Sustainable Energy Reviews*, 60, 284-305 (2016).

Grigorova, M.; Blythe, H. J.; Blaskov, V.; Rusanov, V.; Petkov, V.; Masheva, V. Magnetic properties and Mössbauer spectra of nanosized CoFe₂O₄ powders. *Journal of Magnetism and Magnetic Materials*, 183, 163–172 (1998).

Grylewicz, S. Rapeseed oil methyl esters preparation using heterogeneous catalysts. *Bioresource Technology*, 70, 249-253 (1999).

Hasan, M. M.; Rahman, M. M. Performance and emission characteristics of biodiesel–diesel blend and environmental and economic impacts of biodiesel production: A review. *Renewable and Sustainable Energy Reviews*, 74, 938-948, (2017).

Huixia, F.; Baiyi, C.; Deyi, Z.; Jianqiang, Z.; Lin, T. Preparation and characterization of the cobalt ferrite nanoparticles by reverse coprecipitation. *Journal of Magnetism and Magnetic Materials*, 356, 68–72 (2014).

Hudson, R.; Feng, Y.; Varma, R. S.; Moores, A. Bare magnetic nanoparticles: sustainable synthesis and applications in catalytic organic transformations. *Green Chemistry*, 10, (2014).

Kouzu, M.; Yamanaka, S.; Hidaka, J.; Tsunomori, M. Heterogeneous catalysis of calcium oxide used for transesterification of soybean oil with refluxing methanol. *Applied Catalysis A: General*, 355, 94-99 (2009).

Lu, A. H.; Salabas, E. L.; *Angew. S. Magnetic Nanoparticles: Synthesis, Protection, Funcionalization, and Application. Angewandte Chemie International Edition*, 46, 1222-1244, (2007).

Mardhiah, H. H.; Ong, H. C.; Masjuki, H. H.; Lim, S.; Lee, H. V. A review on latest developments and future prospects of heterogeneous catalyst in biodiesel production from non-edible oils. *Renewable and Sustainable Energy Reviews* 67, 1225-1236 (2017)

Martins, L.; Cardoso, D. Influence of surfactant chain length on basic catalytic properties of Si-MCM-41. *Microporous and Mesoporous Material*, 106, 8-16 (2007).

Mozaffari, M.; Amighian, J.; Darsheshdar, E. Magnetic and structural studies of nickel-substituted cobalt ferrite nanoparticles, synthesized by the sol-gel method. *Journal of Magnetism and Magnetic Materials*, 350, 19-22 (2014).

Nair, P.; Singh, B.; Upadhyay, S.N.; Sharma, Y.C. Synthesis of biodiesel from low FFA waste frying oil using calcium oxide derived from Mererex as a heterogeneous catalyst. *Journal of Cleaner Production* 29, 82-90 (2012).

Polshettiwar, V.; Luque, R.; Fihri, A.; Zhu, H.; Bouhrara, M.; Bassett, J.-M. Magnetically recoverable nanocatalysts. *Chemical Reviews*, 111, 3036-3075, (2011).

Rossi, L. M.; Costa, N. J. S.; Silva, F. P.; Wojcieszak, R. Magnetic nanomaterials in catalysis: advanced catalysts for magnetic separation and beyond. *Green Chemistry* 16, 2906-2933, (2014).

Sheldon, R. A.; Wallau, M.; Arends, I. W. C. E.; Schuchardt, U. Heterogeneous Catalysts for Liquid-Phase Oxidations: Philosophers' Stones or Trojan Horses. *Accounts of Chemical Research*, 31, 485-493 (1998).

Shi, M.; Zhang, P.; Fan, M.; Jiang, Pingping, J.; Dong, Y. Influence of crystal of Fe₂O₃ in magnetism and activity of nanoparticle CaO@Fe₂O₃ for biodiesel production. *Fuel*, 197, 343-347, (2017).

Tang, Z.; Xu, J.; Zhang, J.; Lu, Y. Biodiesel production from vegetable oil by using modified CaO as solid basic catalysts. *Journal of Cleaner Production*, 42, 198-203 (2013).

Taufiq-Yap, Y.H.; Lee, H.V.; Yunus, R.; Juan, J.C. Transesterification of non-edible *Jatropha curcas* oil to biodiesel using binary Ca-Mg mixed oxide catalyst: Effect of stoichiometric composition. *Chemical Engineering Journal*, 178, 342-347 (2011).